

A FUNDAMENTAL STUDY ON SHEAR BOND STRENGTH OF STEEL ENCASED REINFORCED CONCRETE MEMBERS

H. Hotta, H. Kihara, and K. Takiguchi
Department of Architecture and Building Engineering, Tokyo Institute of
Technology, Tokyo, Japan

Abstract

This paper deals with the shear bond strength of steel encased reinforced concrete (SRC) members. A theoretical strength is led based on the upper bound theorem in plastic analysis, assuming idealized deformation and failure surface in members. The proposed formula indicates that the shear bond strength depends on an axial load level, and its adequacy is confirmed empirically. Bond characteristics between encased steel and concrete are also examined empirically, and it is concluded that the influence of the bond cannot be neglected when cross-H shaped steel is encased in the members. Finally, the condition that such a brittle failure can be avoided is reconsidered. Key words: steel encased reinforced concrete, shear bond failure, upper bound theorem, bond characteristics

1 Introduction

Shear-bond failure is a peculiar failure mode in SRC composite. The strength of this failure mode was investigated empirically by Wakabayashi and Minami (1975), and the empirical formula still survives as an AIJ design code for SRC members. However, the strength given by the design formula is rather smaller than the actual one as for the short members and those encasing cross-H shaped steel, that was indicated by Kato (1978), and in our

previous experiment (1991). Therefore the applicable region or the formula itself must be reconsidered.

In this paper, a theoretical shear bond strength of an RC part is proposed, based on the upper bound theorem in limit analysis, and its adequacy is confirmed empirically. As the proposed formula indicates that the shear bond strength is influenced by bond characteristics between steel plate and concrete theoretically, these characteristics are also investigated empirically varying lateral confinement.

Finally, the condition that the members encasing cross-H shaped steel fail due to shear bond failure is considered using the knowledge obtained in the above examinations.

2 Theoretical shear bond strength based on plastic theory

Fig. 1 shows an idealized deflection of the concrete divided into two parts at the center line along its axial direction in a column subjected to an axial load, N , a bending moment, M , and shear force, Q . The column has the section of $B \times D$ and the length of L . In Fig. 1, R is the end rotation of the column, and δ_n is half of the axial displacement. The two blocks of the concrete slip with each other along their contact bounds with the displacement $2\delta_s$.

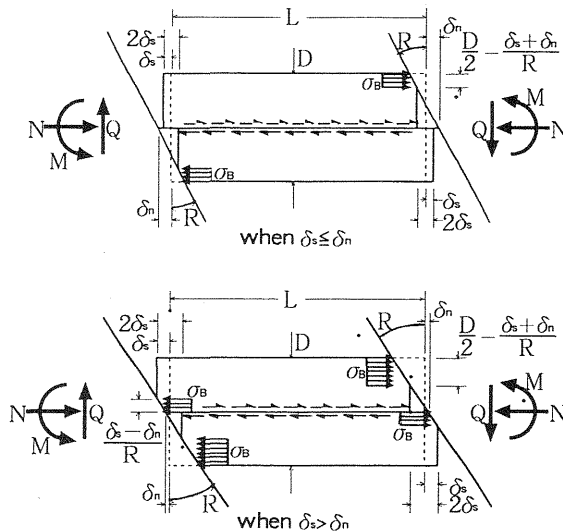


Fig. 1 Idealized deflection of column

Using non-dimensional parameters, $\epsilon_n (= \delta_n / (RD))$, for the axial displacement, δ_n , the work done by the external forces W_e is expressed as:

$$W_e = 2MR - 2N\delta_n = 2(M - ND\epsilon_n)R \quad (1)$$

Assuming that the concrete is a rigid-plastic body having the compressive yield stress, σ_B , and the tensile stress, zero, internal stress distributes as shown in Fig. 1.

Also, using the non-dimensional parameter, $\varepsilon_s (= \delta_s / (RD))$, for δ_s , the equilibrium of the axial force gives:

$$N = \frac{1}{2} BD \sigma_B (1 - 2\varepsilon_s - 2\varepsilon_n) \quad (\delta_s \leq \delta_n) \quad (2a)$$

$$N = \frac{1}{2} BD \sigma_B (1 - 4\varepsilon_n) \quad (\delta_s > \delta_n) \quad (2b)$$

When the slipping along the contact bounds does the work, T , per a unit length due to the friction or the shear failing, and using the non-dimensional parameter, $\alpha (= T / (BD \sigma_B))$, instead of T , the work done by the internal forces W_i is given as follows:

$$\begin{aligned} W_i &= 2 \int_0^{\frac{D}{2} - \frac{\delta_s + \delta_n}{R}} B \sigma_B R x dx + 2T \delta_s \\ &= BD^2 \sigma_B \left\{ \left(\frac{1}{2} - \varepsilon_s - \varepsilon_n \right)^2 + 2\alpha \varepsilon_s \right\} R \quad (\delta_s \leq \delta_n) \quad (3a) \end{aligned}$$

$$\begin{aligned} W_i &= 2 \int_0^{\frac{D}{2} - \frac{\delta_s + \delta_n}{R}} B \sigma_B R x dx + 2 \int_0^{\frac{\delta_s - \delta_n}{R}} B \sigma_B R x dx + 2T \delta_s \\ &= BD^2 \sigma_B \left\{ \left(\frac{1}{2} - \varepsilon_s - \varepsilon_n \right)^2 + (\varepsilon_s - \varepsilon_n)^2 + 2\alpha \varepsilon_s \right\} R \quad (\delta_s > \delta_n) \quad (3b) \end{aligned}$$

In the case of $\delta_s = 0$, the maximum end moment, M_{\max} , can be calculated from the equilibrium of work done by the external and the internal forces $W_e = W_i$, and using Eq.(2a), as

$$M_{\max} = \frac{1}{2} BD^2 \sigma_B n (1 - n), \quad (4)$$

where n is the non-dimensional parameter of the axial load ($n = N / (BD \sigma_B)$). Equation (4) is the same as the well known M-N interaction relationship.

In the case of slipping along the contact bound that does the work T due to the friction or the shear failure of the cover concrete, the maximum end moment, M_{\max} , is given. In the same way as the above explanation, the equation on M_{\max} can be given, however, this equation includes the slipping displacement, ε_s . According to the upper bound theorem, the minimum work done by the internal forces gives the correct answer. Hence the problem is to find ε_s , which minimizes M under the constant axial force, N . Finally, the equations on M_{\max} are given as follows. When $n \leq \alpha$, $\varepsilon_s = 0$ gives the max. moment expressed as:

$$M_{\max} = \frac{1}{2}BD^2\sigma_B n(1-n), \quad (5a)$$

and when $n > \alpha$, $\varepsilon_s = \frac{1}{4} - \frac{\alpha}{2}$ gives the max. one as

$$M_{\max} = \frac{1}{4}BD^2\sigma_B \{n(1-n) + \alpha(1-\alpha)\} \quad (5b)$$

The M-N interaction relationship given as Eqs. (5a) and (5b) are illustrated in Fig. 2. In the case of $\alpha = 0$, drawn by means of a dotted line, both divided concrete bricks behave independently, as any stress is not transferred through a slipping surface. The maximum end moment is just half of the case as they behave together without slipping. In the case of $\alpha \geq 0.5$, members never fail due to shear bond failure mode regardless of axial load ratio. In the case of $0 < \alpha < 0.5$ and $n > \alpha$, they fail due to shear bond failure mode, and the strength is dependent on the axial load ratio. The M-N interaction curves in the case $\alpha = 0.2$ is described as a solid line for the example.

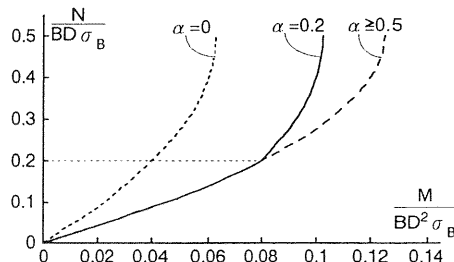


Fig. 2 Proposed M-N interaction curves

3 A verification of theoretical formulas of shear bond strength

3.1 Outline of experiment

Cyclic shear-bending tests were carried out under a constant axial load for the purpose of confirming the adequacy of the proposed formulas. Specimens are steel encased reinforced concrete columns having the section of 160mm × 160mm as shown in Fig. 3. A thin steel plate having a thickness of 3.2mm was used as encased steel. In order to grasp the end moment shared by the concrete exactly, the surface of the flat steel and the longitudinal bars were waxed and greased so that the bond between them and the concrete was removed, and they weren't anchored to the end plate. Therefore, they don't behave as structural elements. All specimens are listed in Table 1. The name of a specimen is composed of [W1 or W2]-[the ratio of effective width of concrete to width of specimen (%)]-[shear span ratio]-[axial force ratio (%)]. The experimental variable of the W1 series is axial force ratio, and that of the W2 series is cover area of concrete that isn't divided by the steel plate and is able to transmit shear force directly.

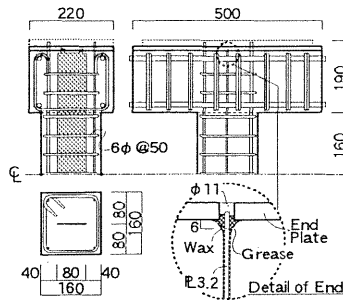


Fig. 3 A typical specimen

Table 1 List of specimens

Name of specimen	Clear length (mm)	Effective-width of concrete (mm)	Axial force (kN)	σ_B (MPa)
W1-25-1-18	320	40	157	34.8
W1-25-1-26			235	
W1-25-1-48			431	
W2-25-1-48	320	40	353	28.8
W2-50-1-48		80		
W2-25-2-48		40		

3.2 Experimental results

End moment-end rotation skeleton curves are shown in Fig. 4. All the specimens had cracked near 0.003rad and failed due to shear bond failure. The maximum shear strength of the W1 series is higher, as axial force ratio is higher. In other words, the shear strength is dependent on the axial load level as the proposed formulas indicate.

W1-25-1-48 and W2-25-1-48 were tested under the same conditions expected for the strength of the concrete. W2-50-1-48 and W2-25-2-48 had the same area of cover concrete and axial load ratio. However, there were meaningful discrepancies between their normalized maximum strength. The reason the above results arose is that the bond between steel and concrete, which might be independent of concrete strength, wasn't removed perfectly.

Fig. 5 shows the experimental results and M-N interaction curves of the proposed theoretical formulas described as a solid line. The values of α are calculated by assuming that the shear strength of concrete is $0.3 \sigma_B$ and the bond strength between steel and concrete is 1MPa. The experimental values are compared with the calculated ones as shown in Table 2. They are in general harmony.

The strength on large deformation is in good agreement with the M-N interaction curve in the case of $\alpha = 0$. This means that slipping failure surface transmits no stress, because cover concrete and the bond are broken and the concrete behaves as two independent parts divided by the steel.

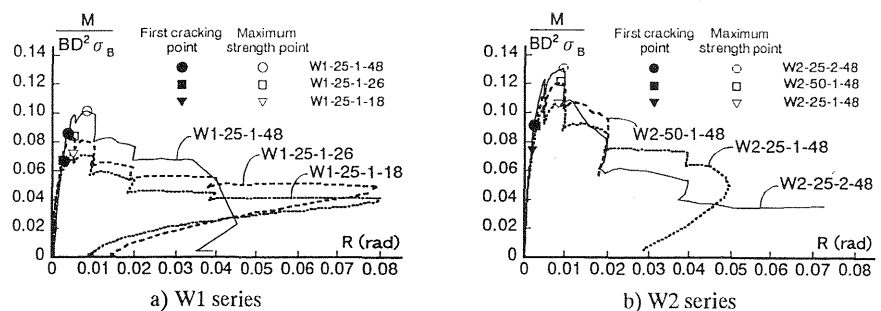


Fig. 4 End moment-end rotation skeleton curves

4.2 Experimental results

Typical testing results, bond stress vs. slipping displacement relations are described in Fig. 7. The higher confinement stress causes the higher maximum bond stress, and the difference between them is almost the same regardless of the slipping displacement. Fig. 8 shows the overall relationships between the bond stress and the lateral confinement stress. The relationships between the max. bond strength and the lateral confinement stress is illustrated with void marks and a solid line, and the bond stress at the displacement of 5mm is illustrated with solid marks and a dashed one. It can be concluded that the compressive strength of concrete does not influence the bond strength at all, and that both the relationships between the bond strengths and the lateral confinement stress are expressed as the following linear equations:

$$\tau_a = 0.283 \sigma_c + 2.30 \quad (\tau_a = \tau_{\max}) \quad (6a)$$

$$\tau_a = 0.296 \sigma_c + 1.29 \quad (s=0.5\text{mm}) \quad (6b)$$

Thus the second term of the above equations, which means the bond strength, changes according to the slipping displacement. However, the first term, which means the friction, is not dependent on the slipping displacement, and the friction coefficient is about 0.29.

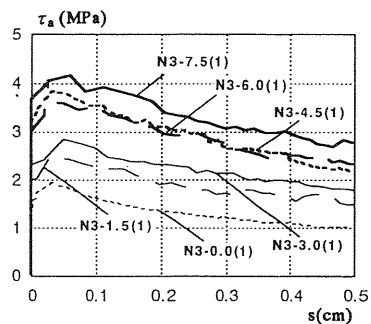


Fig. 7 A typical bond stress-slip displacement curves

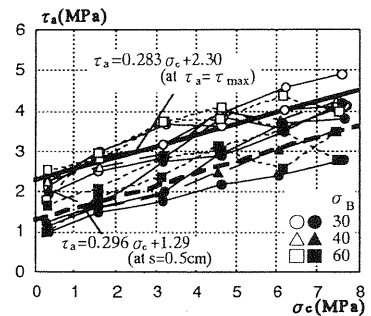


Fig. 8 Relationship between bond and confining stress

5 Shear bond strength of SRC columns encasing cross-H shaped steel

5.1 Outline of experiment

Four specimens listed in Table 4 were made and tested. They were all SRC members encasing cross-H shaped steel, the section of which is indicated in Fig. 9. The variable was clear length of the specimens.

Similarly to the experiment explained in Chapter 2, the ends of the embedded steel and the longitudinal bars were not anchored to the end plate. The bars were also waxed and greased in order to grasp the end moment

shared by the concrete accurately. The surface of the steel plate, however, was not treated and it maintained the sound bond characteristic. The purpose of this examination is to grasp the influence of the bond stress on the shear strength. Under a constant axial load of 360kN ($0.42BD \sigma_b$), cyclic shear bending tests were carried out.

Table 4 List of specimens

Name of specimen	Clear length (mm)	σ_b (MPa)	Steel section (mm)
CH-320-BO	320	32.4	CrossH-130 × 30 × 3.2 × 3.2
CH-520-BO	520	31.8	
CH-640-BO	640	34.2	
CH-880-BO	880		

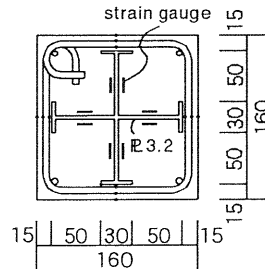


Fig. 9 A typical cross section

5.2 Experimental Results

End moment vs. end rotation skeleton curves of all specimens are described in Fig. 10. Only the shortest specimen with the length of 320mm failed due to shear bond failure mode. The others failed due to bending. The end moment reached the calculated one and the strength almost did not degrade until they deformed considerably. If no bond exists between the steel and the concrete at all, the lower limit length of the specimen that fails due to bending is 120cm. The bond obviously affects the shear strength, and a bond stress of about 0.5MPa must be considered assuming the uniform distribution of the bond stress.

Even when the members fail due to bending at first, shear bond failure is able to occur after yielding because the shear strength of the cover concrete decreases according to the growth of flexural plastic hinge zone at both ends. However, the degradation of the strength has never been observed in specimens that failed due to bending. It is further proof that the bond is concerned.

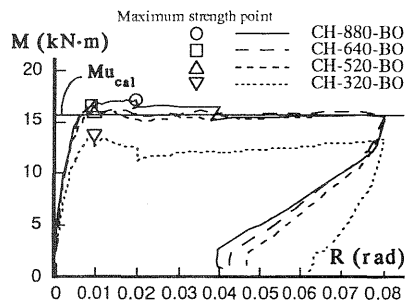


Fig. 10 End moment-end rotation skeleton curves

Fig. 11 shows the typical histories of axial and lateral strain of encased steel measured in the tests. Although the strain at the center of the specimen was almost constant regardless of the end rotation, the one at the end still increased after yielding. It can be said that the shear strength of the cover concrete at the hinge zone decreases according to the growth of the hinge zone. However, the bond strength is sound at the hinge zone.

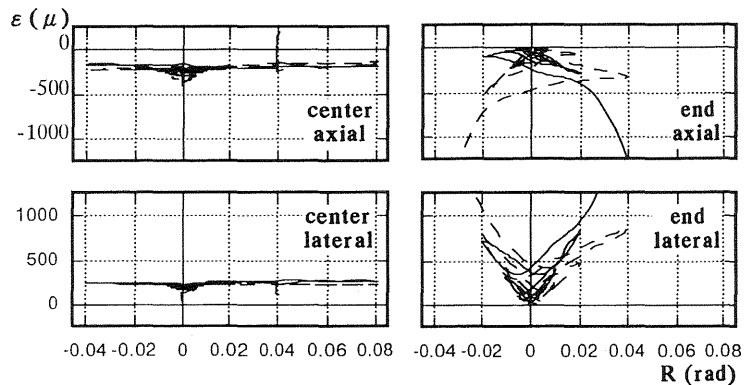


Fig. 11 Histories of axial and lateral strain of steel

6 Conclusions

1. Shear bond strength of RC parts in SRC members is well estimated by the proposed formula expressed as Eqs.(5a) and (5b).
2. Shear bond strength of SRC members is dependent on axial load as the proposed formula indicates.
3. The relationship between bond strength and lateral confinement stress is linear, and it is given as Eq.(6a) regardless of the compressive strength of concrete.
4. Bond characteristic greatly affects shear bond strength of SRC members, in the case where cross-H shaped steel is encased.

References

- Architectural Inst. of Japan (AIJ) (1987) **Standard for structural calculation of steel reinforced concrete structures.**
- Hotta, H., Chen, Z. and Takiguchi, K. (1995) Shear-transferring Mechanism of Steel-Hoop-Concrete Column, **Proc. of the 5th East Asia-Pacific Conf. on Struct. Engng. and Constr.**, 1, 627-632.

- Hotta, H., Kihara, H. and Takiguchi, K. (1997) An empirical study on shear strength of steel encased reinforced concrete members concerning bond stress between steel and concrete. **Journal of Struct. Constr. Engng. AIJ**, 493, 131-137.
- Hotta, H., Kihara, H. and Takiguchi, K. (1998) Shear strength of SRC member concerning bond stress between steel and concrete. **Proc. of the 6th East Asia-Pacific Conf. on Struct. Engng. and Constr.**, 1, 641-646.
- Kato, B. and Shohara, R. (1978) Strength of steel-reinforced concrete members. **Transactions of Architectural Inst. of Japan**, 266, 19-29.
- Suzuki, T., Takiguchi, K., Hotta, H., Igarashi, T. and Kato, M. (1991) Shearing behavior of steel-hoop-concrete column. **Journal of Struct. Constr. Engng. AIJ**, 430, 31-39.
- Suzuki, T., Takiguchi, K. and Hotta, H. (1992) Shear Strength of Steel-Hoop-Concrete Composite Column, **Proc. of the 10th World Conference on Earthquake Engineering**, 6, 3461-3466.
- Wakabayashi, M. and Minami, K. (1975) Shear strength of steel reinforced concrete columns under constant axial load and well-defined alternately repeated bending and shear. **Concrete Journal**, 13, 3, 1-17.